

Heteroblastic Development of Transfer Cells Is Controlled by the microRNA miR156/SPL Module¹[OPEN]

Suong T. T. Nguyen, Teighan Greaves, and David W. McCurdy*

Centre for Plant Science, School of Environmental and Life Sciences, The University of Newcastle, Callaghan, NSW 2308, Australia

ORCID IDs: 0000-0002-4997-9649 (S.T.T.N.); 0000-0003-2083-7783 (D.W.M).

We report that wall ingrowth deposition in phloem parenchyma (PP) transfer cells (TCs) in leaf veins of *Arabidopsis thaliana* represents a novel trait of heteroblasty. Development of PP TCs involves extensive deposition of wall ingrowths adjacent to cells of the sieve element/companion cell complex. These PP TCs potentially facilitate phloem loading by enhancing efflux of symplasmic Suc for subsequent active uptake into cells of the sieve element/companion cell complex. PP TCs with extensive wall ingrowths are ubiquitous in mature cotyledons and juvenile leaves, but dramatically less so in mature adult leaves, an observation consistent with PP TC development reflecting vegetative phase change (VPC) in *Arabidopsis*. Consistent with this conclusion, the abundance of PP TCs with extensive wall ingrowths varied across rosette development in three ecotypes displaying differing durations of juvenile phase, and extensive deposition of wall ingrowths was observed in rejuvenated leaves following prolonged defoliation. PP TC development across juvenile, transition, and adult leaves correlated positively with levels of miR156, a major regulator of VPC in plants, and corresponding changes in wall ingrowth deposition were observed when miR156 was overexpressed or its activity suppressed by target mimicry. Analysis of plants carrying miR156-resistant forms of *SQUAMOSA PROMOTER BINDING PROTEIN LIKE* (*SPL*) genes showed that wall ingrowth deposition was increased in *SPL9*-group but not *SPL3*-group genes, indicating that *SPL9*-group genes may function as negative regulators of wall ingrowth deposition in PP TCs. Collectively, our results point to wall ingrowth deposition in PP TCs being under control of the genetic program regulating VPC.

Transfer cells (TCs) play critical roles in membrane transport of solutes at various sites within plants and between plants and their environment (Gunning and Pate, 1969; Offler et al., 2003; McCurdy, 2015). This transport capacity is conferred by wall protuberances that extend into the cell lumen, hence called wall “ingrowths”. These ingrowths, considered to be primary wall-like in composition (Vaughn et al., 2007), are deposited secondarily on the inner face of the primary cell wall and function to enhance the area of surrounding plasma membrane, therefore increasing surface-to-volume ratio of the TC and consequently promoting potential transmembrane flux of solutes

(Gunning et al., 1968; Gunning and Pate, 1974; Offler et al., 2003).

TCs have been reported widely across the plant kingdom, from seedless plants, e.g. algae, hornworts, mosses, etc., to gymnosperms and angiosperms, including both monocotyledons and dicotyledons (Gunning and Pate, 1969; Pate and Gunning, 1972; Gunning, 1977; Offler et al., 2003). Across the plant kingdom, the occurrence of TCs is proposed to be an indicator of anatomical locations where intensive transport occurs; however, the existence of bottlenecks in nutrient exchange does not always ensure development of TC morphology. In fava bean (*Vicia faba*) seeds, for example, TCs develop in both maternal and filial interfaces while they are present at just the filial site of corn (*Zea mays*) seeds and completely absent in seeds of string bean (*Phaseolus vulgaris*; Offler et al., 2003). Interestingly, many species lacking TCs under normal growth conditions nonetheless have the capacity to produce these highly specialized cells when abnormal stimuli or stress are applied; an example of this scenario is where iron and phosphorous starvation bring about wall ingrowth formation in rhizodermal TCs of tomato (*Solanum lycopersicum*; Schikora and Schmidt, 2002). A compilation of such sporadic but versatile and widespread occurrences of TCs suggests that all plant species possess the genetic information coding for their development, but this genetic competency may be repressed in some circumstances (Gunning and Pate, 1974; Gunning, 1977). This observation has raised a

¹ Funding for this work was provided to D.W.M. by the Australian Research Council (Discovery Project no. DP110100770) and the Faculty of Science and Information Technology, University of Newcastle. S.T.T.N. was supported by a VIED scholarship from the Vietnam Ministry of Agriculture and Rural Development.

* Address correspondence to david.mccurdy@newcastle.edu.au.

The author responsible for distribution of materials integral to the findings presented in this article in accordance with the policy described in the Instructions for Authors (www.plantphysiol.org) is: David McCurdy (david.mccurdy@newcastle.edu.au).

D.W.M. and S.T.T.N. conceived and designed the experiments; S.T.T.N. and T.G. performed the experiments; S.T.T.N., T.G., and D.W.M. analyzed the data; S.T.T.N. and D.W.M. wrote the article. All authors approved the final manuscript.

[OPEN] Articles can be viewed without a subscription.

www.plantphysiol.org/cgi/doi/10.1104/pp.16.01741

long-standing question of why and when a given tissue of a given species develops TCs with wall ingrowths if its genome encodes capacity to do so. This question implies that specific signals are required for TC development and thus response to these signals may vary depending on the developmental context of the tissue or its exposure to specific biotic or abiotic stresses.

In *Arabidopsis* (*Arabidopsis thaliana*), phloem parenchyma (PP) cells in the minor vein network of leaves (Haritatos et al., 2000) and sepals (Chen et al., 2012) can develop wall ingrowths to become PP TCs. Wall ingrowths in these PP TCs are typically bulky and predominantly abut sieve elements (SEs) and to a lesser extent companion cells (CCs; Haritatos et al., 2000; Amiard et al., 2007). PP TCs have been assumed to facilitate the efflux of photoassimilates into the apoplasm (Haritatos et al., 2000), and support for this notion was the recent discovery of SWEET11 and 12 effluxers in plasma membrane putatively associated with wall ingrowths in these PP TCs (Chen et al., 2012).

Previous studies of PP TCs in *Arabidopsis* veins have relied on using transmission electron microscopy (TEM) because these cells are buried deep within vascular bundles (e.g. Haritatos et al., 2000; Amiard et al., 2007; Maeda et al., 2006, 2008). Recently, we used a modified pseudo-Schiff-propidium iodide (mPS-PI) procedure for staining cell walls (Truernit et al., 2008; Wuyts et al., 2010) to image wall ingrowth deposition in PP TCs by confocal microscopy (Nguyen and McCurdy, 2015). This procedure enables more extensive and semiquantitative assessment of PP TC development at the whole leaf level and across rosette development compared to using TEM, and was used to assess, among other criteria, the extent of wall ingrowth deposition in response to defoliation (Nguyen and McCurdy, 2015). In surveying PP TCs across individual leaf and rosette development, we identified that wall ingrowth deposition was highly abundant in early emerged organs such as cotyledons (Nguyen and McCurdy, 2015) and juvenile leaves, and was dramatically less so in later-emerged adult leaves. These observations led us to speculate that PP TC development, as assessed by levels of wall ingrowth deposition, is specific to leaf identity.

Leaf identity is specified during shoot development through heteroblasty or vegetative phase change (VPC), a phenomenon where plants progress from a juvenile, to transition, and then an adult phase (Poethig, 1990; Kerstetter and Poethig, 1998). The progression of phase transition is mainly controlled by miR156-mediated repression of *SQUAMOSA PROMOTER BINDING PROTEIN LIKE* (*SPL*) genes, with this class of *SPL* involved in promoting a variety of adult traits (Wu and Poethig, 2006). In addition, a small subset of VPC traits are regulated by a second pathway, the transacting-small-interfering RNA/AUXIN RESPONSE FACTOR-dependent pathway (Hunter et al., 2006). In this study, we investigated the hypothesis that PP TC development is regulated by the same genetic program, or elements thereof, that control VPC. We found

that levels of miR156 across leaf maturation of both juvenile and adult leaves correlated strongly with PP TC development, and conversely, levels of the miR156 target genes, namely *SPL3*, *SPL9*, *SPL10*, and *SPL15*, showed a negative correlation with wall ingrowth deposition in PP TCs. Furthermore, disrupting VPC by either extensive defoliation or genetic manipulation of the miR156-*SPL*-specific pathway caused corresponding changes in levels of wall ingrowth deposition. Collectively, we conclude that PP TC development is controlled by the genetic program that regulates VPC in *Arabidopsis*. The implications of this finding in terms of the putative role(s) for PP TCs in *Arabidopsis* veins are discussed.

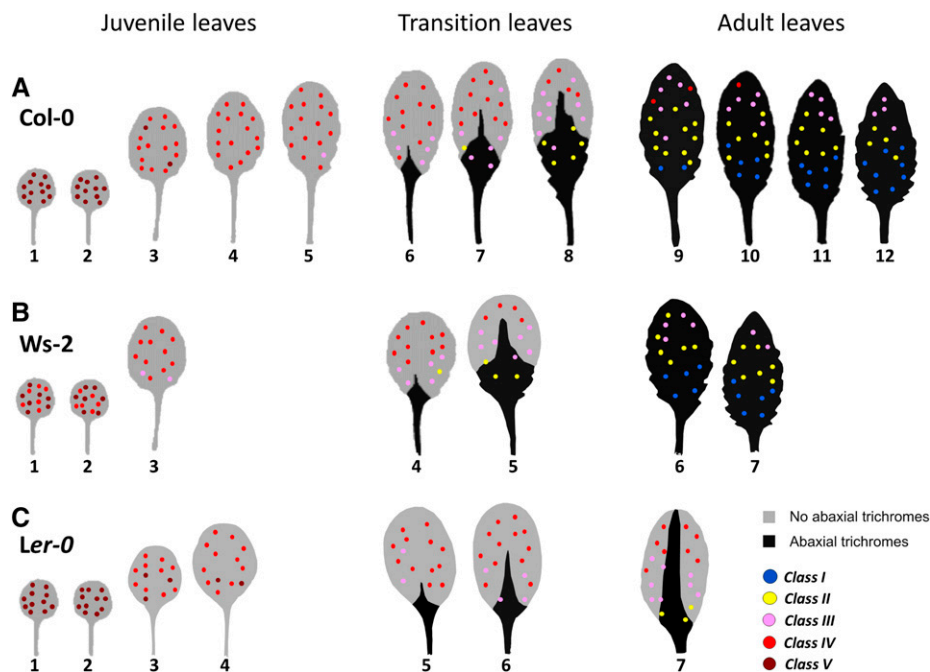
RESULTS

Classification and Observations of Wall Ingrowth Abundance in PP TCs of *Arabidopsis* Veins

We recently reported semiquantitative assessment of wall ingrowth deposition in PP TCs of *Arabidopsis* veins by confocal imaging of leaves stained by a modified pseudo-Schiff propidium iodide staining technique (Nguyen and McCurdy, 2015). This article described four classes of PP TC development depending on abundance of wall ingrowth deposition, ranging from Class I with no wall ingrowths to Class IV with abundant deposition (Nguyen and McCurdy, 2015). By assigning an arbitrary value of 0, 2, 4, and 6 for Classes I, II, III, and IV, respectively, a semiquantitative assessment of wall ingrowth deposition in PP TCs across single leaves of developing and developed shoots could be generated (Nguyen and McCurdy, 2015). Following extensive observations of PP TCs in organs such as cotyledons and early juvenile leaves in this study, we have added an additional Class V (8 points) to this scoring system, whereby Class V PP TCs show massively abundant wall ingrowth deposition that occupies a substantial volume of the PP TC. This extended classification scheme is outlined in Supplemental Figure S1 and scoring of wall ingrowth deposition based upon this modified scheme was performed as described in Nguyen and McCurdy (2015). Based on this scheme, and herein, we use the term "PP TC development" to indicate levels of wall ingrowth deposition in these cells.

A survey of PP TC development at the whole leaf level throughout shoot development in *Arabidopsis* ecotype Columbia-0 (Col-0) revealed that early emerged juvenile leaves have abundant Class IV or V PP TCs distributed throughout the entire vein system, whereas in later-emerged adult leaves, PP TCs are much less abundant (Class II or III) and are distributed across the leaf in a distinctive basipetal gradient (Fig. 1A). Early transition leaves have relatively numerous Class IV PP TCs, whereas in late transition leaves PP TCs are predominantly Class III and display the basipetal gradient similar to the patterns seen in adult leaves (Fig. 1A).

Figure 1. Heteroblastic development of PP TCs in ecotypes Col-0, Ws-2, and Ler-0. A, PP TC abundance and distribution in mature leaves 1 to 12 from 30-d-old Col-0 plants ($n = 9$). B, PP TC abundance and distribution in mature leaves 1 to 7 from 25-d-old Ws-2 plants ($n = 4$). C, PP TC abundance and distribution in mature leaves 1 to 7 from 28-d-old Ler-0 plants ($n = 4$). The colored dots in A to C represent PP TC development across each leaf as defined by Classes I to V (see Supplemental Fig. S1). Leaf template images were modified from Yang et al. (2013).



Collectively, in a mature plant, successive leaves differ in levels of PP TC development, with these levels gradually decreasing along the shoot axis (Fig. 1A). These observations are consistent with PP TC development representing, to our knowledge, a novel trait of heteroblasty in Arabidopsis, and thus encouraged us to further investigate heteroblastic features of PP TC development.

PP TC Development and Distribution in Mature Rosette Leaves Reflect Heteroblastic Differences Among Ecotypes

Telfer et al. (1997) reported that the ecotypes Col-0, Landsberg *erecta* (*Ler*), and Wassilewskja (*Ws*) display differing durations of juvenile phase. Therefore, we examined if changes in PP TC development in these ecotypes also reflects differences in heteroblasty accordingly. Under long-d conditions, abaxial trichomes frequently appeared in leaf 6 of Col-0, leaf 4 of Ws-2, and leaf 5 of *Ler-0* plants (Supplemental Fig. S2A). Leaves lacking abaxial trichomes are juvenile leaves, whereas leaves partially or completely covered with abaxial trichomes are defined as transition or adult leaves, respectively (Telfer et al., 1997; Willmann and Poethig, 2011). We noted that in Col-0, leaves 6 to 8 are transition leaves and leaves 9 to 12 are adult (Fig. 1A), whereas in Ws-2, leaves 4 and 5 are transition and leaves 6 and 7 are adult (Fig. 1B). The latest-emerged leaves 12 and 7 of Col-0 and Ws-2 plants, respectively, are typical of adult identity with hundreds of trichomes covering the whole abaxial leaf surface (Supplemental Fig. S2A). In *Ler-0* plants, however, and in most instances, the latest-emerged leaf 7 has many fewer abaxial trichomes, which were frequently restricted to the

midvein, making them more like transition leaves (Fig. 1C; Supplemental Fig. S2A).

Interestingly, PP TC development and distribution in leaf veins of all three ecotypes showed a negative correlation with that of abaxial trichomes. In mature juvenile leaves 1 and 2, which do not have abaxial trichomes, PP TCs with extensive wall ingrowth deposition (Class V for Col-0 and *Ler-0*, Classes IV and V for Ws-2) were extremely abundant and distributed throughout the whole leaf vein system (Figs. 1 and 2, A, E, and I). Transition leaves in all three ecotypes frequently had Class IV PP TCs distributed across the apical half of the leaf and Class II to IV in basal regions of the leaf (Figs. 1 and 2, B, F, and J). Latest emerged adult leaves 11 and 12 of Col-0 plants and leaf 7 of Ws-2 plants, which are completely covered by abaxial trichomes at maturity, had many fewer PP TCs with mostly Class II or III at the tip region, Class I or II in the middle third of the leaf, and Class I at the base of the leaf (Figs. 1 and 2, C, D, G and H). Latest emerged adult leaf 7 of *Ler-0* plants, which were partially covered by abaxial trichomes, had abundant PP TCs with Class IV at the tip, Class III in the middle, and Class II or III at the base (Figs. 1 and 2, K and L). The gradual decrease and eventual absence of PP TCs in the basal region of last-emerged adult leaves in Col-0 (Fig. 1A) and Ws-2 (Fig. 1B) is concomitant with a significant decrease in cell size, particularly cells of vascular bundles including PP cells (Supplemental Fig. S2B).

Although total leaf number of Ws-2 and *Ler-0* plants were similar (6 or 7 leaves), there were striking differences in wall ingrowth deposition in PP TCs between leaf 6 of these two ecotypes, and these differences paralleled differences seen in abaxial trichome abundance

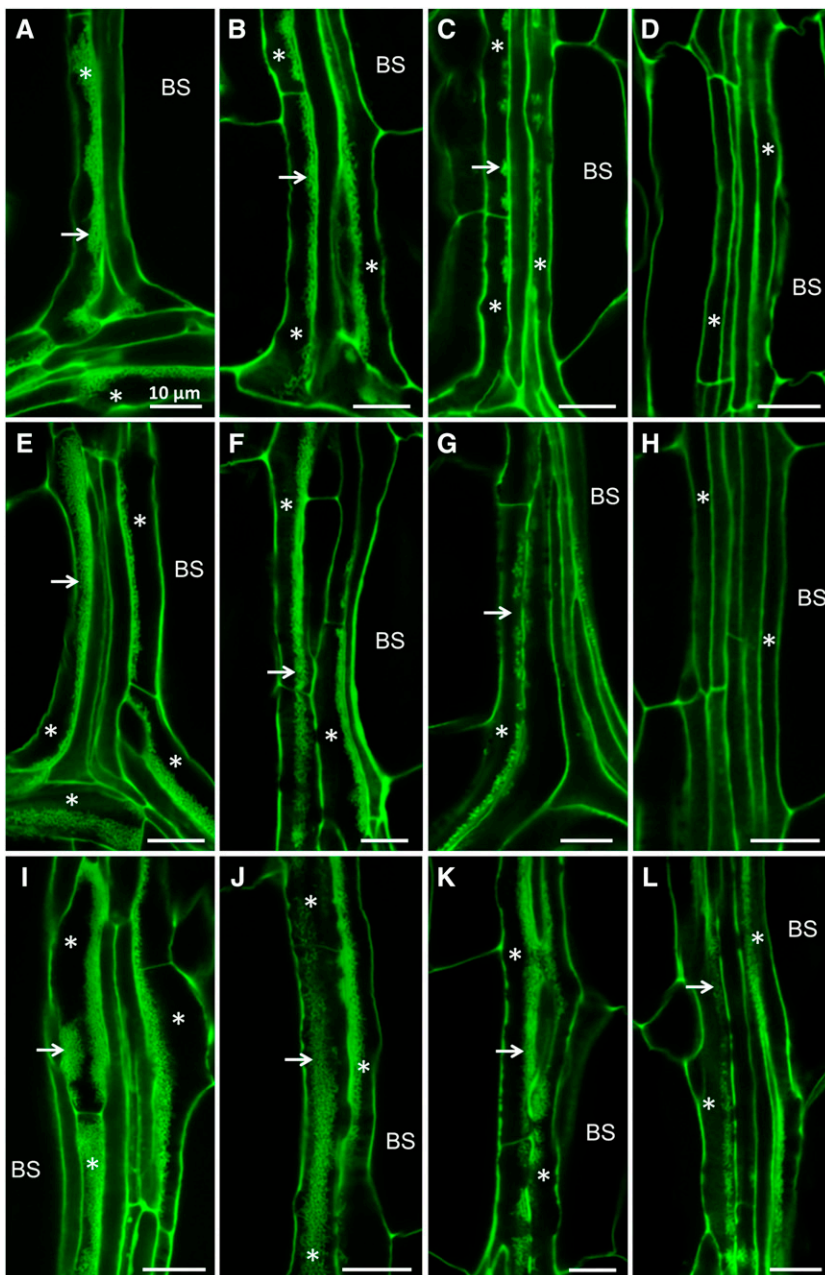


Figure 2. Confocal imaging of wall ingrowth deposition in PP TCs in mature leaves of different ecotypes. A to D, Col-0. E to H, Ws-2. I to L, Ler-0. A, E, and I, Confocal images of veins from juvenile leaf 1 of Col-0 (A), Ws-2 (E), and Ler-0 (I) plants showing Class V PP TCs characterized by massive deposition of wall ingrowths (arrows) occupying a large volume of each PP TC (asterisks). B, F, and J, Confocal images of veins from transition leaves, namely leaf 6 of Col-0 (B), leaf 4 of Ws-2 (F), and leaf 6 of Ler-0 (J) plants, showing Class IV PP TCs with extensive deposition of wall ingrowths (arrows). C, D, G, H, K and L, Confocal images of veins from adult leaves, namely leaf 11 of Col-0 (C and D), leaf 6 of Ws-2 (G and H), and leaf 7 of Ler-0 (K and L). Adult leaves of Col-0 and Ws-2 have Class III PP TCs (asterisks) with clusters of wall ingrowths (arrows) at the leaf tip (C and G) and have PP cells (asterisks) without wall ingrowths at the leaf base (D and H). Class IV PP TCs are seen at the leaf tip (K) and Class III PP TCs at the leaf base (L) in adult leaf 7 of Ler-0. Scale bar = 10 μm for all images. BS, bundle sheath.

and distribution. Leaf 6 of Ws-2 plants was typical of adult leaves with numerous abaxial trichomes distributed across the entire leaf (Fig. 1B; Supplemental Fig. S2). Consistently, PP TCs in these leaves also showed adult characteristics with Class III PP TCs at the tip (Figs. 1B and 2G) and declining to Class I or II at the base (Figs. 1B and 2H), which resembled PP TCs in adult leaves 10 or 11 of Col-0 plants (Fig. 1A). PP TCs in leaf 6 of Ler-0 plants, however, showed typical transition characteristics with Class IV observed throughout the vein network except for a few basal regions containing Class III PP TCs (Figs. 1C and 2J). Abaxial trichomes in these leaves were few in number and restricted to the midvein (Fig. 1C; Supplemental Fig. S2A). Also, leaf 6 of Ws-2 plants was

highly serrated whereas leaf 6 of Ler-0 plants displayed smooth margins (Supplemental Fig. S2). These results collectively support the conclusion that PP TC development differed across ecotypes in Arabidopsis in a manner similar to the known differences in vegetative phase length among these ecotypes.

Defoliation Confirms that Abundant PP TCs with Extensive Wall Ingrowth Deposition Signify Juvenile Identity of Leaves

It is well established that defoliation and severe pruning (Njoku, 1956; Libby and Hood, 1976; Yang et al., 2011), or culture of adult shoot apices in low-sugar

medium (Orkwiszewski and Poethig, 2000), prolongs the production of juvenile traits in both herbaceous and woody plants. In this study, we performed prolonged defoliation to examine if PP TC development occurs as part of whole-shoot rejuvenation. Ten-d-old plants were subjected to leaf ablation where leaves 1 and 2 were removed (Fig. 3A), and this process of leaf removal was continued at 2- or 3-d intervals until a total of eight leaves were ablated. Defoliated plants subsequently displayed a prolonged juvenile phase and produced approximately seven more juvenile leaves than control plants, but had a normal adult phase duration (Fig. 3B). Leaves 9 and 10 in control plants showed typical adult characteristics with numerous abaxial trichomes, short petioles, and elongated, serrated, and highly down-curved blades, whereas leaves produced at comparable nodes in defoliated plants were completely rejuvenated, evidenced by the absence of abaxial trichomes (Fig. 3C), long petioles, and round, smooth, and flat blades, resembling leaves 3 or 4 of control plants (Fig. 3, D and E). In addition to these external morphological changes, internal anatomy of leaves 9 and 10 of defoliated plants also strikingly mirrored juvenile identity, evidenced by simple venation patterns and larger cell size (Supplemental Fig. S3). Of significance to this study, PP TC development in rejuvenated leaf 10, akin to PP TC development in juvenile leaves, was dramatically increased compared to that in leaf 10 of control plants (Fig. 3, F to K). In addition, the distribution of PP TCs with abundant wall ingrowths did not display a basipetal gradient seen in control leaf 10, but rather was uniformly abundant from tip to base in these rejuvenated leaves (Fig. 3, I and J). Collectively, these results show that changes in PP TC development paralleled changes in other phase-specific traits upon defoliation and that rejuvenated leaves displayed juvenile-like wall ingrowth deposition, thus indicating that abundant PP TCs with extensive wall ingrowths signify juvenile identity of leaves.

PP TC Development Across Leaf Maturation Varies Depending on Heteroblastic Status of the Leaf and Is Independent of Day Length

In *Arabidopsis*, differentiated PP cells, characterized by a smooth primary cell wall, transdifferentiate to form PP TCs with wall ingrowths in vascular bundles of leaves and leaf-like organs (Haritatos et al., 2000; Nguyen and McCurdy, 2015, 2016). The striking differences in PP TC development between juvenile and adult leaves at their maturity (Figs. 1 and 2, A, C, D, E, G, and H) imply differences in the transdifferentiation process of PP TCs in these leaves. Therefore, we examined the process of PP TC development across leaf maturation from expanding to fully expanded leaves. Our analysis of expanding leaves revealed that, regardless of leaf identity, PP TC fate was not determined during the ontogeny of vascular cells. Procambial cells, differentiating from the meristem, can follow either

phloem or xylem cell fates to form phloem or xylem cell precursors, respectively. Phloem cell precursors then differentiate into SEs, CCs, or PP cells (Fukuda, 2004; Schuetz et al., 2013). Therefore, the presence of SEs with distinct sieve plates can serve as an indicator of the differentiated state of other phloem cells. As shown in Figure 4, A to C, PP cells in vascular bundles of early expanding juvenile, transition, and adult leaves are fully differentiated, similar to SEs with characteristic sieve plates, but because their primary walls appear smooth, similar to neighboring CCs, these PP cells have not formed papillate wall ingrowths. These expanding leaves are normally less than 20% (v/v) of their final size, and therefore can be considered as immature leaves.

Later in leaf development, PP cells express a second cell fate when they transdifferentiate to become PP TCs. The initiation of this process is the same in expanding juvenile, transition, and adult leaves, as evidenced by the appearance of distinctive wall ingrowth material on the inner surface of the primary cell wall adjacent to cells of the SE/CC complex (Fig. 4, A' to C'). However, the ongoing process of building extensive networks of wall ingrowths was strikingly different among leaf identities, with this process occurring very rapidly across the maturation of juvenile leaves (Figs. 2, A, E, and I, and 4D), but notably slower in transition leaves and strikingly slower in adult leaves (Figs. 2, C, D, G, and H, and 4D). Significantly, we observed no major differences in xylem development, as revealed by mPS-PI staining, among mature juvenile, transition, and adult leaves (Supplemental Fig. S4), indicating that the differences seen in PP TC development at these different developmental states is a VPC-specific phenomenon.

We also examined heteroblastic development of PP TCs under short-day conditions, given that the onset of abaxial trichomes, the marker of VPC, is delayed in short-day plants (Telfer et al., 1997). By eight weeks, short-day Col-0 plants had produced at least 34 visible leaves ($n = 12$) and had 13 or 14 juvenile leaves ($n = 4$), with these leaves bearing no abaxial trichomes, having long petioles, smooth leaf margins, and rounder leaf blades (Supplemental Fig. S5A; compare to Figure 1A and Supplemental Fig. S2). Wall ingrowth deposition in PP TCs also displayed juvenile characteristics in these leaves, namely an increased abundance in leaves 7 and 10 compared to that in long-day grown plants, and absence of a basipetal gradient of PP TC development in leaf 10 (Supplemental Fig. S5B). These results demonstrate that PP TC development reflects the heteroblastic status of leaves, regardless of day length.

Strong Correlations Between Levels of miR156 and its *SPL* Targets and PP TC Development across Leaf, Shoot, and Basipetal Maturation in Adult Leaves

Because our data to this point was consistent with the interpretation that wall ingrowth deposition in PP TCs

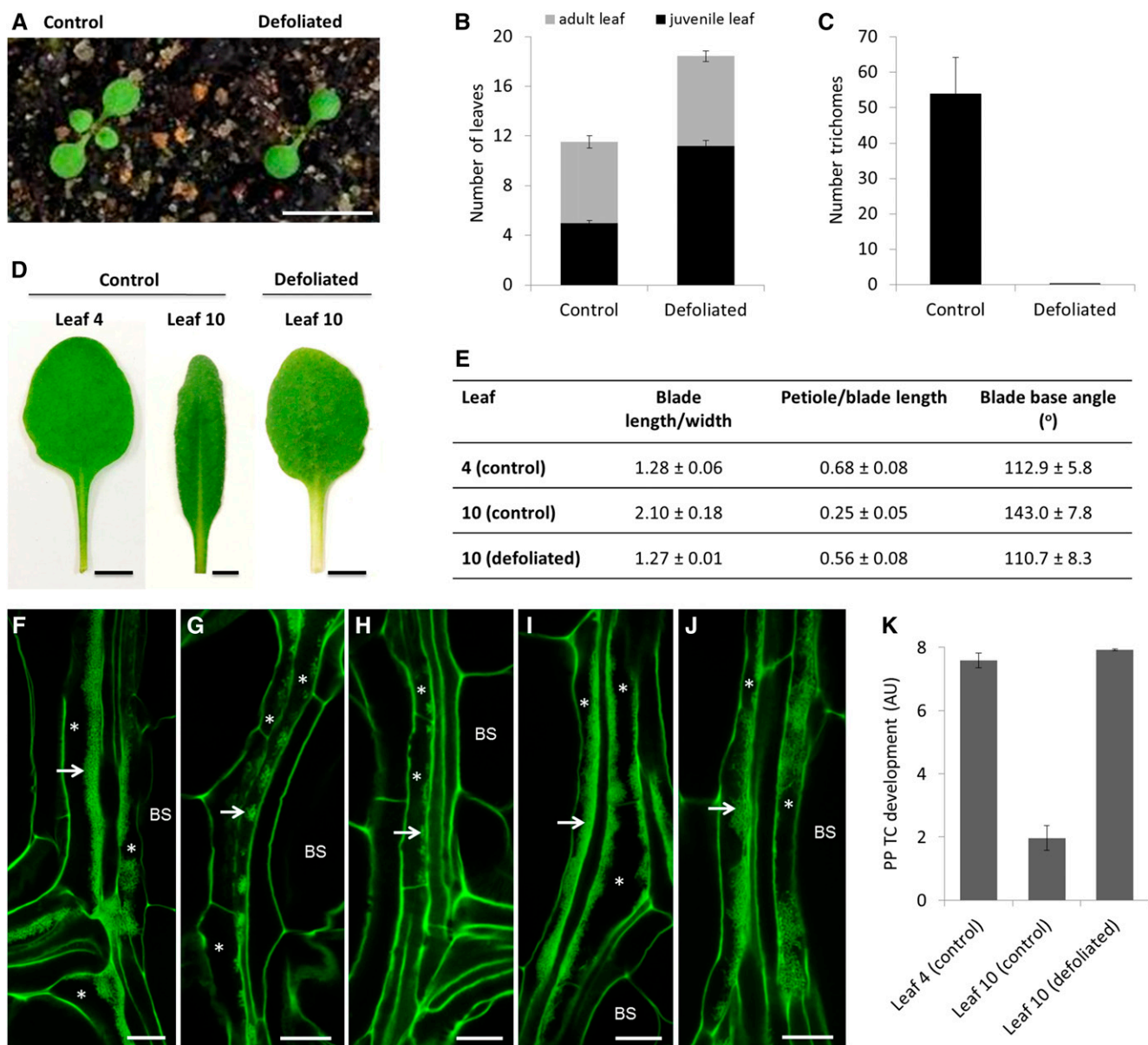


Figure 3. Effects of prolonged defoliation on PP TC development. A, Ten-d-old Col-0 seedlings before and after defoliation of juvenile leaves 1 and 2. Scale bar = 10 mm. B, Numbers of juvenile and adult leaves from control and defoliated plants. Leaf ablation delayed the production of adult leaves in defoliated plants; these plants produced approximately seven more juvenile leaves than control plants but the number of adult leaves was unaffected. Data are mean \pm SE ($n = 12$). C, Leaf 10 of defoliated plants was completely rejuvenated, evidenced by the absence of abaxial trichomes. Data are mean \pm SE ($n = 12$). D and E, Morphology of rejuvenated leaf 10 of defoliated plants resembled that of juvenile leaf 4 of control plants in terms of long petiole, round blade, and narrower blade base angles, whereas leaf 10 of control plants was typical of adult characteristics with elongated blade, short petiole, and wide blade base angles. Scale bars = 5 mm for all images in (D). F to J, Confocal imaging of wall ingrowth deposition in PP TCs in mature leaves. Class V PP TCs with massive deposition of wall ingrowths were observed in both apical (I) and basal (J) regions of rejuvenated leaf 10 from defoliated plants, which is akin to PP TC development in leaf 4 of control plants (F). In contrast, leaf 10 of control plants had Class III PP TCs at the tip (G) and Class II PP TCs at the base (H). Arrows point to wall ingrowths; asterisks indicate PP TCs. Scale bars = 10 μ m in all panels. K, Semiquantitative analysis of PP TC development in rejuvenated leaf 10 of defoliated plants compared to leaves 4 and 10 of control plants. Defoliation experiments were performed three times ($n = 9$, $n = 10$, and $n = 12$) with the same outcomes. Results from one experiment are presented. BS, bundle sheath.

may be a component of the phase change program and hence potentially under the same genetic control as VPC, we examined changes in the abundance of the miR156 sRNA and expression of its target genes under

the conditions where changes in PP TC development were observed. The miR156 levels were measured by stem-loop RT-qPCR in representative juvenile (3 or 4), transition (7), and adult (11 or 12) leaves in mature

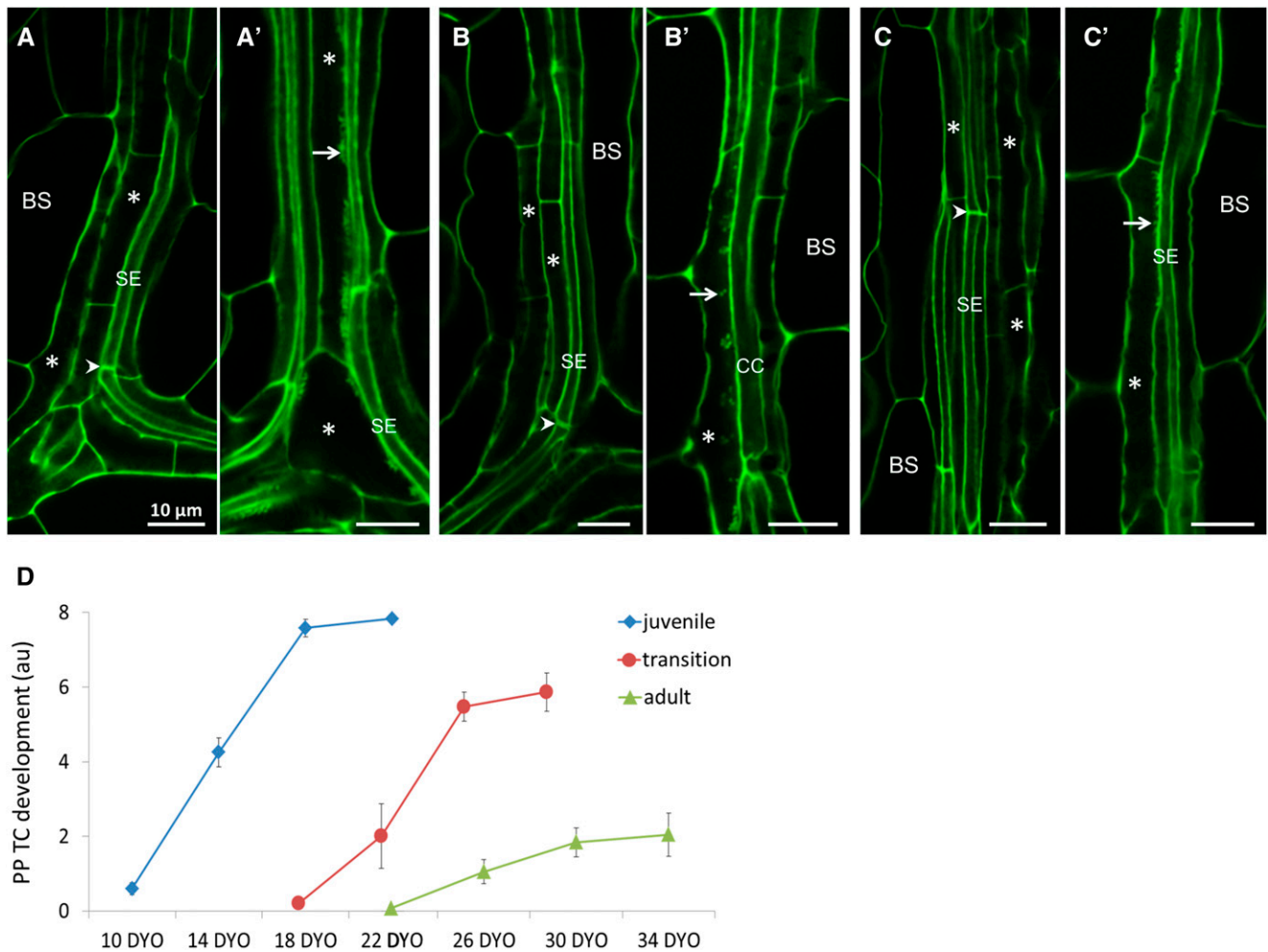


Figure 4. PP TC development across leaf maturation in relation to differentiation of SEs. A to C, Confocal images of veins from juvenile leaf 1 (A), transition leaf 6 (B), and adult leaf 11 (C) at their immature stage. These immature leaves had not developed PP TCs with wall ingrowths, evidenced by smooth cell walls of PP cells (asterisks); note that SEs were well differentiated, indicated by the presence of sieve plates (arrowheads). A' to C', Confocal images of veins from juvenile leaf 1 (A'), transition leaf 6 (B'), and adult leaf 11 (C') at their intermediate stages. PP cells in these leaves had transdifferentiated to become PP TCs (asterisks), evidenced by wall ingrowth papillae or small clusters of wall ingrowths (arrows) adjacent to SEs and/or CCs. Arrows point to wall ingrowth deposition; arrowheads indicate sieve plates; asterisks indicate PP cells or PP TCs. Scale bars = 10 μ m in all images. D, Profiles of PP TC development across maturation of each juvenile, transition, and adult leaf identity. BS, bundle sheath; DYO, day-old.

(32-d-old) *Arabidopsis* shoots. Consistent with previous reports showing that miR156 levels at the whole shoot level decrease with shoot age (Wang et al., 2009; Wu et al., 2009), our data showed that in mature shoots, concomitant with a decrease in PP TC development (Fig. 5A), miR156 levels decreased 1.7- and 2.2-fold in transition and adult leaves, respectively, compared to that in juvenile leaves (Fig. 5B). Concomitant with a decline in miR156 abundance, the expression of several of its target genes, including *SPL3*, *SPL9*, *SPL10*, and *SPL15*, increased consistently across the juvenile to adult transition, with *SPL15* showing the strongest response to decreased miR156 abundance (Fig. 5B). An increase in abundance across the juvenile to adult transition was also observed for miR172 (Fig. 5B), a

positive regulator of VPC (Wu et al., 2009). Collectively, these results demonstrate correlations between miR156 sRNA abundance, miR156 target gene expression, and PP TC development in mature leaves (Fig. 5, A and B), thus strongly implying a role for miR156 in promoting wall ingrowth deposition in PP TCs during the juvenile phase.

To examine if the abundance of miR156, and that of its target genes, across individual leaf maturation also correlated with changes in wall ingrowth deposition in PP TCs, we measured their levels in representative juvenile leaf 1, and adult leaf 11, at different stages of maturation of each leaf. Leaves 1 and 11 were sampled from 11-, 17-, and 23-d-old, or 23-, 29-, and 35-d old plants, respectively, representing immature, intermediate, and mature status of these juvenile or adult

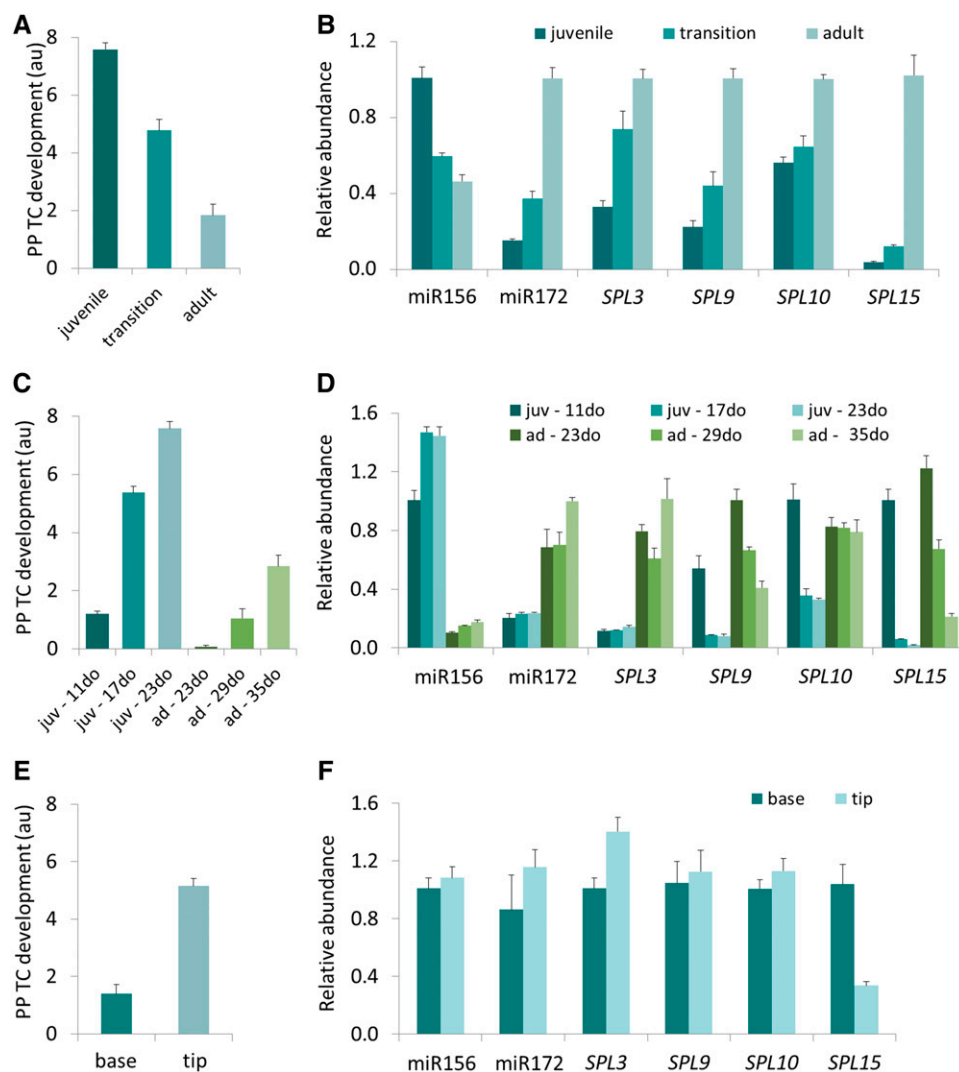


Figure 5. Strong correlations among PP TC development and abundance of miR156, miR172, and *SPLs*. A, C, and E, PP TC development across shoot maturation (A), leaf maturation of juvenile leaf 1 and adult leaf 11 (C), and basipetal maturation in adult leaf 11 (E). B, D, and F, RT-qPCR analysis of transcripts isolated from leaves at the same developmental stages as leaves subjected to mPS-PI staining and PP TC analysis as shown in A, C, and E, accordingly. Relative abundance levels were set to 1 for: miR156 in juvenile leaves and miR172, *SPL3*, *SPL9*, *SPL10*, and *SPL15* in adult leaves (B); miR156, *SPL10*, and *SPL15* in 11-d-old leaf 1, miR172, and *SPL3* in 35-d-old adult leaf 11, and *SPL9* in 23-d-old adult leaf 11 (D); and miR156, miR172, *SPL3*, *SPL9*, *SPL10*, and *SPL15* in apical regions of adult leaf 11 (F). Data are mean \pm SE across at least five biological replicates for A, B, C, E, and F, and three biological replicates for D. juv, juvenile; ad, adult.

leaves. Consistent with an increase in PP TC development across leaf maturation (Fig. 5C), miR156 levels increased significantly from immature to intermediate and mature status, in both juvenile and adult leaves, with consistently higher miR156 abundance in juvenile leaves compared to adult leaves at the same maturation status of each leaf (i.e. immature juvenile versus immature adult leaves, etc.; Fig. 5D). *SPL9* and *SPL15* expression showed an opposite pattern, that is, both transcripts were reduced in their abundance from immature to mature status for both juvenile and adult leaves, with their levels consistently lower in juvenile leaves compared to adult leaves at the same maturation status of each leaf (Fig. 5D). Interestingly, the most dramatic changes were again observed for *SPL15*, with transcript levels of this gene decreasing by 55-fold across immature to mature transition of juvenile leaf 11, and 5.7-fold across the same transition for adult leaf 11 (Fig. 5D). *SPL10* levels reduced across maturation of juvenile leaves but remained unchanged across maturation of adult leaves, while *SPL3* expression and miR172 abundance showed a similar trend, namely being stable

during maturation of juvenile leaves but increasing from immature and intermediate to mature status in adult leaves (Fig. 5D). Again, these observations link temporal changes in wall ingrowth abundance in PP TCs to temporal changes in molecular phenotype of known regulators of VPC, including miR156, *SPL9*, and *SPL15*, during the maturation of individual leaves (Fig. 5, C and D).

Given the distinct distributions of PP TCs between the tip and base of adult leaves (Figs. 1, 2, and 5E), we next assessed the levels of miR156 and miR172 and the *SPLs* in these regions. The apical third, and basal third (excluding the major vein), of leaf 11 were dissected and subjected to expression analysis. There was a 1.4-fold increase in *SPL3* levels but no significant change in the abundance of miR156, miR172, *SPL9*, and *SPL10*. However, *SPL15* expression was reduced by 3.1-fold in the apical third, compared to the basal third (Fig. 5F), a finding that further strengthens the tight negative correlation observed for PP TC development and *SPL15* expression (Fig. 5, A to D).

Altered Heteroblastic Development of PP TCs in Leaf Veins of *sqn-6*, *35S::MIM156* and *35S::MIR156* Plants Strongly Correlate with Altered Levels of miR156 and Its Target Genes

The strong correlation between PP TC development and miR156 abundance indicated a role for miR156 in regulating PP TC development. Therefore, we next examined PP TC development in Arabidopsis plant lines modified to have alterations in the miR156/*SPL* expression module. Numerous plant lines harboring mutations in the miRNA pathway, including *hasty* (Telfer and Poethig, 1998), *squint* (*sqn*; Berardini et al., 2001), *serrate* (Clarke et al., 1999), and *hyponastic leaves1* (Lu and Fedoroff, 2000), have a shortened juvenile phase attributed to decreased miR156 abundance (Park et al., 2005; Lobbes et al., 2006; Li et al., 2012) or its activity (Smith et al., 2009). Additionally, some of these mutants also display altered reproductive competence and/or flowering time (Telfer and Poethig, 1998; Lu and Fedoroff, 2000). Several vegetative phase-specific traits are affected by floral induction (Willmann and Poethig, 2011), and it can be highly challenging in some instances to distinguish between flowering-dependent and flowering-independent effects on leaf morphology/anatomy. The Arabidopsis *sqn* mutant, a plant line defective in the activity of cyclophilin 40, displays altered vegetative phase transition, but flowering time and reproductive competence remains unchanged (Berardini et al., 2001). Therefore, to specifically examine effects of VPC on heteroblastic features of PP TC development, we analyzed PP TC development in leaf veins of the *sqn-6* allele. In addition to flowering at almost the same time as Col-0 plants, but with fewer leaves, *sqn-6* plants showed a precocious adult vegetative phenotype evidenced by an early appearance of abaxial trichomes and leaf margin serration (Supplemental Fig. S6, A and B; see also Berardini et al., 2001; Usami et al., 2009). Leaf 5 of 30-d-old Col-0 plants displayed typical juvenile characteristics, namely the absence of abaxial trichomes and Class IV or V PP TCs seen in a majority of minor veins across the whole leaf (Figs. 1A and 6A). By comparison, PP TC development in leaf 5 of 30-d-old *sqn-6* plants was significantly reduced, with this reduction being more obvious in the basal region of leaves (Fig. 6A), consistent with these leaves attaining a precocious adult vegetative phenotype (Supplemental Fig. S6C). PP TCs with extensive wall ingrowths were very abundant in the first two leaves of *sqn-6* plants (Supplemental Fig. S6, D and E), again in agreement with these leaves retaining juvenile identity (Supplemental Fig. S6A). This result is consistent with the heteroblastic status of PP TC development being independent of d length (Supplemental Fig. S5).

Constitutive expression of a miR156 target mimic transgene in Col-0 plants results in these plants, *35S::MIM156*, displaying a severely altered VPC with precocious appearance of adultlike leaves replacing the juvenile phase (Franco-Zorrilla et al., 2007). In our study, leaves 1 and 2 of *35S::MIM156* plants developed

typical adultlike features, including abaxial trichomes (Supplemental Table S1), serrated leaf margins, and large and elongated blades (Supplemental Fig. S7, A and C). However, inconsistent with previous reports (Franco-Zorrilla et al., 2007; Todesco et al., 2010), many of these plants flowered earlier than Col-0 and this flowering phenotype was frequently seen in plants with a reduced number of leaves (Supplemental Fig. S7A). Further, a considerable variation in leaf number was observed across the population of *35S::MIM156* plants assessed, ranging from 2 to 4 leaves (strong phenotype), 5 to 7 leaves (mild phenotype), or 8 to 9 leaves (weak phenotype), with the mild phenotype predominating (Supplemental Fig. S7). We chose leaf 5 from 30-d-old *35S::MIM156* plants exhibiting the mild phenotype (5 to 7 leaves in total) to examine altered heteroblastic development of PP TCs in more detail. These leaves showed typical adult characteristics with numerous abaxial trichomes (Supplemental Table S1) and elongated blades (Supplemental Fig. S7D). PP TC development in minor veins of *35S::MIM156* plants was significantly reduced compared to leaf 5 of Col-0 plants at the same developmental stage (Fig. 6A), with this difference being more pronounced in the basal half of these leaves (Fig. 6A).

Overexpression of the miR156 precursor transcript greatly elevates miR156 levels and prolongs the juvenile phase of *35S::MIR156a* plants, as evidenced by production of significantly more leaves displaying juvenile traits, including a lack of abaxial trichomes, long petioles, and round and small-sized leaf blades (Schwab et al., 2005; Wu and Poethig, 2006). Leaf 10 of 35-d-old *35S::MIR156a* plants (Wu and Poethig, 2006) showed typical juvenile characteristics, whereas leaf 10 of 35-d-old Col-0 plants exhibited adult morphology (Supplemental Fig. S7E). In agreement with extensive wall ingrowth deposition signifying juvenile identity, we found a significant increase in PP TC development in veins of leaf 10 from *35S::MIR156a* plants compared to that of Col-0, with this difference being most obvious in the basal half of the assessed leaves (Fig. 6A).

Levels of miR156 and its *SPL* targets have previously been measured in *sqn-1* and *sqn-6* mutants as well as *35S::MIM156* and *35S::MIR156a* plants; however, these measurements were made using whole seedlings and/or inflorescence tissues (Franco-Zorrilla et al., 2007; Smith et al., 2009), or pooled leaves from different nodes (Franco-Zorrilla et al., 2007; Usami et al., 2009). To more accurately correlate miR156 and *SPL* levels with PP TC abundance, we quantified miR156 accumulation, the expression of miR156 target genes *SPL3*, *SPL9*, *SPL10*, and *SPL15*, and miR172 abundance in: (1) leaf 5 from 30-d-old *sqn-6*, *35S::MIM156*, and Col-0 plants, and (2) leaf 10 from 35-d-old *35S::MIR156a* and Col-0 plants. Consistent with the findings of Smith et al. (2009) and Usami et al. (2009), our data showed no significant change in miR156 levels in the *sqn-6* mutant compared to Col-0, but *SPL3*, *SPL9*, and *SPL15* levels were elevated 2.4-, 2.6-, and 4-fold, respectively, in leaf 5 of

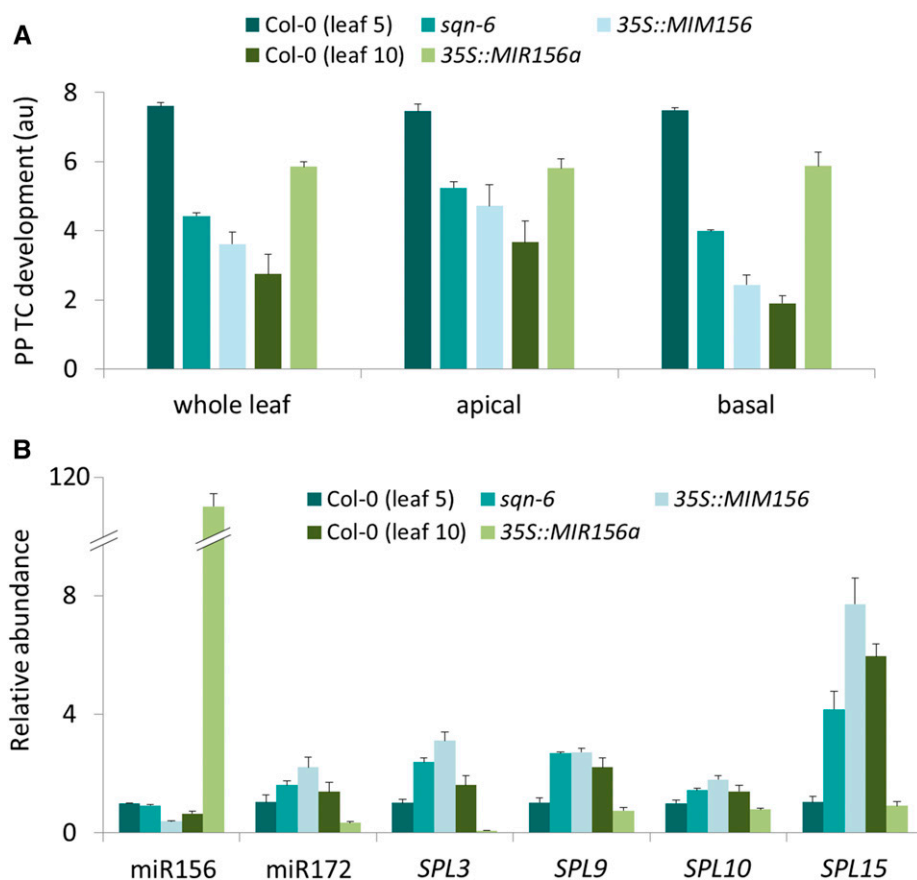


Figure 6. Effects of *sqn-6*, miR156 target-site mimic, and overexpression of miR156 on PP TC development. A, PP TC development in leaf 5 of 30-d-old plants was reduced in *sqn-6* and *35S::MIM156* (target-site mimic) lines compared to Col-0, whereas it was increased in leaf 10 of 35-d-old plants in *35S::MIR156a* (overexpression) relative to Col-0. Effects on PP TC development were more significant in the basal-third compared to the apical-third of leaves. B, RT-qPCR analysis of transcripts isolated from leaves at the same developmental stages as leaves subjected to mPS-PI staining and PP TC analysis as shown in A. Relative abundance was set to 1 for leaf 5 of Col-0 for all transcripts. Data are mean \pm se across at least four biological replicates.

30-d-old *sqn-6* plants (Fig. 6B). This finding implies that the *sqn* mutation had major effects on miR156 activity, rather than influencing the level of this sRNA (Smith et al., 2009). The miR156 target-site mimic caused a 2.6-fold reduction in miR156 levels in leaf 5 of *35S::MIM156* compared to the same leaf of Col-0 plants, and we subsequently demonstrate that this reduction in miR156 abundance led to significant increases in levels of all examined *SPLs*, and miR172 abundance. Again, the most dramatic change was observed for *SPL15* expression (7.4-fold increase; Fig. 6B). These changes are in agreement with the appearance of precocious adult features observed in PP TC development. The increase in miR156 abundance and corresponding decrease in miR172 and *SPL* levels in leaf 10 of *35S::MIR156a* plants overexpressing miR156 (Fig. 6B) is consistent with the juvenilized phenotype of PP TC development seen in this leaf (Fig. 6A).

***SPL9*-Group, but Not *SPL3*-Group Genes, Regulate Heteroblastic Development of PP TCs in Leaf Veins**

The consistently observed negative correlation between *SPL* levels and PP TC development suggested that these transcripts may negatively control heteroblastic development of PP TCs in leaf veins. In Arabidopsis, miR156-targeted *SPLs* can be divided into two

broad classes, represented by *SPL3* (including *SPL3*, *SPL4*, and *SPL5*) and *SPL9* (including *SPL2*, *SPL6*, *SPL9*, *SPL10*, *SPL11*, *SPL13*, and *SPL15*; Xing et al., 2010). We examined PP TC development in transgenic plants overexpressing miR156-resistant *SPL3*, *SPL9* and *SPL10*, namely *Pro-35S::rSPL3* (*rSPL3*), *ProSPL9::rSPL9* (*rSPL9*), and *ProSPL10::rSPL10* (*rSPL10*), respectively (Wu and Poethig, 2006; Wang et al., 2008). PP TC development was significantly decreased in leaf 5 of *rSPL9* and *rSPL10* plants, which display precocious expression of all adult-specific leaf traits (Wu et al., 2009). However, this was not observed in *rSPL3* plants compared to Col-0 (Fig. 7A). We also examined PP TC abundance in the gain-of-function mutant *SPL15-1D*, which has a C to T substitution in the miR156 target site of *SPL15* that results in increased expression of *SPL15* and hence a precocious adult phenotype (Usami et al., 2009). PP TC abundance in leaf 5 of *SPL15-1D* plants was significantly reduced compared to Col-0 (Fig. 7A), suggesting a negative role for *SPL15* in regulating wall ingrowth deposition in PP TCs. This hypothesis is supported by the inverse correlation of *SPL15* levels in circumstances where PP TC development was found to be altered accordingly (Figs. 5 and 6). Consistent with redundant effects of *SPL9* and *SPL15* in regulating vegetative phase transition and other aspects of plant development (Schwarz et al., 2008; Wang et al., 2008; Wu et al., 2009), we found no significant effect on PP TC

development in *spl9-4* and *spl15-1* single mutants compared to the significant increase detected in leaf 10 of the *spl9-4/spl15-1* double mutant compared to Col-0 (Fig. 7B). This increase in PP TC abundance in the double mutant was lower than that caused by overexpression of miR156 (*35S::MIR156a*; Fig. 6A), implying that other miR156 targeted *SPLs* may also contribute to repression of wall ingrowth deposition in PP TCs.

Heteroblastic Development of PP TCs Is Unaffected in *zip*, *rdr6*, and *sgs3*

Unlike *sqn* mutations, in which the effects on VPC encompass both the onset of abaxial trichome production and total number of rosette leaves, another class of juvenile-to-adult transition mutations, including *ZIPPY* [an allele of *ARGONAUTE7 (zip)*], *RNA DEPENDENT RNA POLYMERASE 6 (rdr6)*, and *SUPPRESSOR OF GENE SILENCING3 (sgs3)*, involved in the *tasiARF* pathway, accelerate the appearance of adult traits without altering total leaf number due to absence of effects on the length of the transition zone (Hunter et al.,

2003; Peragine et al., 2004; Hunter et al., 2006). We examined if these mutations also showed altered heteroblastic development of PP TCs. Consistent with previous reports (Hunter et al., 2003; Peragine et al., 2004), *zip-2*, *rdr6-11*, and *sgs3-11* mutants exhibited precocious adult vegetative traits such as an elongated and highly down-curved blade of leaves 1 and 2 in 15-d-old plants (Supplemental Fig. S8A), and accelerated abaxial trichome production (Supplemental Fig. S8B). Leaf 5 of these mutants displayed precocious adult features in several traits such as early appearance of abaxial trichomes, increased blade length-to-width ratio, and slightly down-curved blades, but were not altered in other traits including leaf margin serration and blade base angle (data not shown). PP TC development in leaf 5 of these mutants was also not significantly different from that in leaf 5 of Col-0 plants (Fig. 8A), suggesting that *zip-2*, *rdr6-11*, and *sgs3-11* have little to no effect on heteroblastic development of PP TCs. This observation is consistent with a role for *SPL9*-group, but not *SPL3*-group genes, in repressing PP TCs development, as we found that levels of *SPL3* increased 2.9- and 1.5-fold in leaf 5 of *zip-2* and *sgs3-11*, respectively, but levels of miR156, *SPL9*, and *SPL15* did not significantly change (Fig. 8B). Hunter et al. (2006) also reported that these mutations affected only a small subset of heteroblastic traits.

DISCUSSION

Heteroblastic Development of PP TC Wall Ingrowths Is Under Genetic Control of Phase Change

In this study, we have documented, to our knowledge, the novel finding that PP TC development in Arabidopsis leaf veins, as defined by the extent of wall ingrowth deposition, occurs across shoot development in a manner reflecting heteroblasty (Fig. 1), and that this process is under control of the same genetic program regulating VPC. This conclusion is based on our observations demonstrating that changes in PP TC development paralleled changes in leaf abaxial trichomes and other well-defined phase-specific traits defining VPC in a predictable and coordinated manner across normal shoot ontogeny (Figs. 1 and 2), as well as in conditions where shoot progression through ontogeny was delayed because of defoliation (Fig. 3). Furthermore, wall ingrowth deposition in PP TCs was altered in mutants and genetically modified plant lines having altered VPC, namely decreasing in abundance in mutants showing precocious adult phenotypes and increasing in abundance in mutants displaying juvenilized phenotypes (Figs. 6A and 7). Finally, measurements of the expression of miR156 and its *SPL* targets, the key players in genetic pathways regulating VPC, showed strong correlations, both positive and negative, respectively, between the abundance of these transcripts and that of wall ingrowth deposition in PP TCs. In all cases, miR156 levels were high in individual

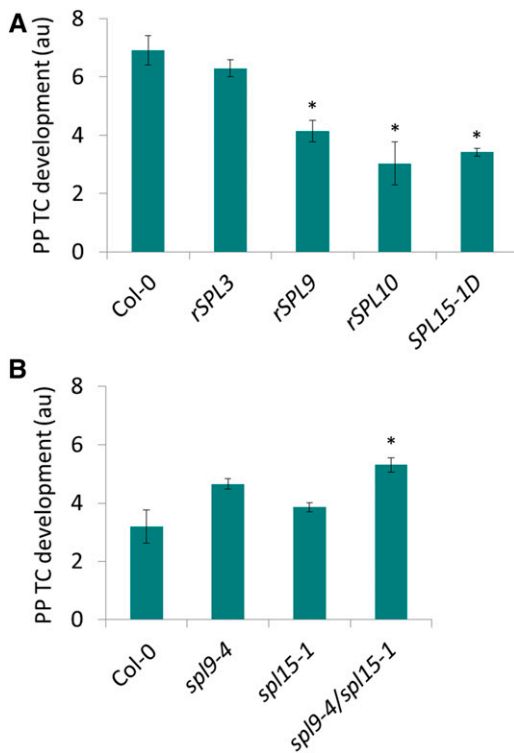


Figure 7. Effects of overexpression of *SPL3*, *SPL9*, *SPL10*, and *SPL15*, and of *spl9-4*, *spl15-1*, and *spl9-4/spl15-1* mutants, on PP TC development. A, PP TC development was reduced in leaf 5 of 30-d-old *rSPL9*, *rSPL10*, and *SPL15-1D* plants but was not significantly affected in *rSPL3* compared to Col-0 ($P < 0.01$, Student's *t* test). B, *spl9-4* and *spl15-1* single mutants did not show significant difference from Col-0 levels, whereas the *spl9-4/spl15-1* double mutant showed a significant increase in PP TC development compared to Col-0 ($P < 0.01$, Student's *t* test). Data are mean \pm SE across three or four biological replicates.

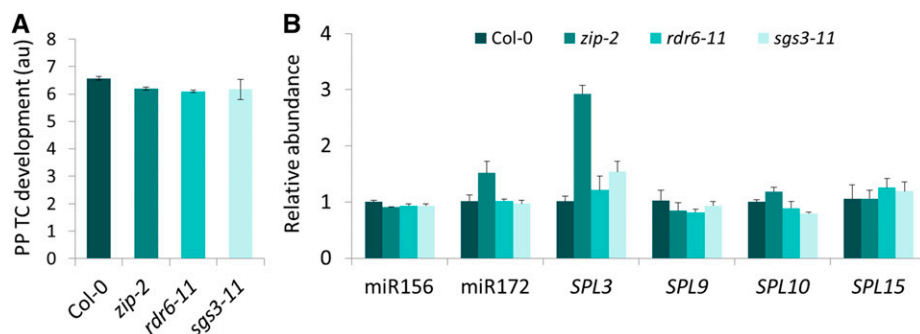


Figure 8. PP TC development was unaffected in *zip-2*, *rdr6-11*, and *sgs3-11* mutants. A, In precocious adult leaf 5 of 30-d-old *zip-2*, *rdr6-11*, and *sgs3-11* mutants, PP TC development showed typical juvenile characteristics with extensive wall ingrowths, similar to that in juvenile leaf 5 of Col-0. B, RT-qPCR analysis of transcripts isolated from leaves at the same developmental stages as leaves subjected to mPS-PI staining and PP TC analysis as shown in A. Relative abundance was set to 1 for leaf 5 of Col-0 for all transcripts. Data are mean \pm SE across four biological replicates.

leaves where wall ingrowth deposition was abundant and low in conditions where wall ingrowth deposition was reduced or less developed. Significantly, the reverse correlation held true for the relationship between wall ingrowth abundance and levels of *SPL9*, *SPL10*, and *SPL15*, and to a lesser extent *SPL3* and *miR172* (Figs. 5, A to D, 6 and 8). Collectively, these observations suggest that extensive wall ingrowth deposition signifies juvenile identity of leaves and that *miR156*, which is both necessary and sufficient for the expression of juvenile traits (Wu et al., 2009), promotes wall ingrowth deposition in PP TCs by repressing *SPLs* expression in the juvenile phase of shoot maturation. Importantly, the absence of apparent differences in xylem development across leaves of different vegetative phase identity (Supplemental Fig. S4) supports the conclusion that the responses seen in PP TC development represent a cell wall deposition event specifically reflecting leaf identity.

Temporal Changes in *miR156* and *SPL* Expression Identify *SPLs* as Repressors of PP TC Development

In agreement with levels of *miR156* being high in young seedlings and gradually decreasing with plant age (Wu et al., 2009; Xu et al., 2016a, 2016b), we found that in mature shoots, juvenile leaves had significantly higher levels of *miR156* compared to *miR156* levels in transition and adult leaves (Fig. 5B). This result is also in agreement with *miR156* levels examined in leaves of Cole's wattle (*Acacia colei*; Wang et al., 2011), rice (*Oryza sativa*; Xie et al., 2006, 2012), and soybean (*Glycine max*; Yoshikawa et al., 2013). In individual leaves, however, *miR156* levels increased during maturation of either juvenile or adult leaves (Fig. 5D); this finding implies that *miR156* levels in a given leaf, at a certain stage of development, is determined by both shoot age (i.e. the node of the leaf in the rosette) and leaf age.

Such temporal changes in *miR156* levels led to a corresponding change in the abundance of the targeted

SPLs (Fig. 5, B and D). Changes in *SPL9* and *SPL15* expression, and to a lesser extent *SPL10*, were opposite to those seen for PP TC development, during both shoot (Fig. 5, A and B) and leaf (Fig. 5, C and D) maturation, implying a repressive role for these *SPLs* in temporally regulating PP TC development. *SPL* proteins are generally classified as transcriptional activators; however, in several cases they can act as transcriptional repressors. For example, *SPL9* indirectly binds to the promoter of *DIHYDROFLAVONOL REDUCTASE*, a key enzyme in anthocyanin biosynthesis, repressing its expression and consequently leading to reduced anthocyanin accumulation (Gou et al., 2011). *SPL9* and *SPL10* have also been shown to directly bind to the transactivation domains of *B-type ARABIDOPSIS RESPONSE REGULATORS (ARRs)*, which encode transcriptional activators of the cytokinin signaling pathway, thereby exerting a role in reducing the regenerative capacity of shoots (Zhang et al., 2015). Schwarz et al. (2008) also postulated that *SPL9* and *SPL15* may negatively regulate leaf maturation rate, consistent with our observation that levels of these two *SPL* transcripts decreased over leaf maturation in both juvenile and adult leaves (Fig. 5D). Collectively, these observations are consistent with *SPLs*, especially *SPL9* and *SPL15*, functioning as negative regulators of PP TC development.

SPL9-group genes have also been shown to function in flowering time (Wang et al., 2009; Wu et al., 2009), with *SPL15* playing a more important role than other *SPL* genes under long-d conditions (Xu et al., 2016a, 2016b). In addition, other components of the flowering pathways including *FLOWERING LOCUS C (FLC)* and *FLOWERING LOCUS T*, also have effects on VPC and leaf morphology, and these effects can be either flowering-dependent or -independent (Willman and Poethig, 2011). Deng et al. (2011) have shown that *FLC* exerts its role in delaying the progression of VPC by binding to the promoter of *SPL15* and thus repress its expression. These observations collectively imply the existence of complex interactions between vegetative and reproductive phase transitions that influence the

development of VPC-specific traits (Willman and Poethig, 2011), and suggest the possibility that heteroblastic development of PP TCs could be affected by floral induction in addition to vegetative maturation. However, our results showing reduced PP TC development in the *sqn-6* mutant (Fig. 6A; Supplemental Fig. S6), and that plants grown under short-d, non-photoinductive conditions, displayed the same heteroblastic development compared to that of abaxial trichomes (Supplemental Fig. S5), argues that PP TC development is tightly coupled to VPC. These results, however, do not formally rule out a role for floral induction on heteroblastic development of PP TCs, but this possibility, mediated by *SPLs* or other factor(s) such as *FLC*, awaits further investigation.

Transdifferentiation of PP TCs and Shoot Regenerative Capacity—Possible Connections via the miR156-*SPL9* Module

The differentiation of PP TCs, like that for most TCs, occurs via transdifferentiation (Offler et al., 2003; Nguyen and McCurdy, 2016), which is defined as an irreversible conversion of a differentiated cell type into another cell type with distinct functional and morphological features (Okada, 1991). The clear reduction in PP TC development in adult leaves compared to juvenile leaves (Fig. 4), implies that the capacity to transdifferentiate into PP TCs is repressed in a majority of PP cells in adult leaves, particularly in cells at the base of the leaf. Interestingly, the transdifferentiation capacity of *Zinnia* (*Zinnia*) mesophyll cells into tracheary elements was also shown to depend on the identity of leaves from which mesophyll cells were isolated (Fukuda and Komamine, 1980). When adult leaves of *Zinnia* plants were used, the transdifferentiation of tracheary elements occurred on d 6 of culture with just 10% of isolated cells forming tracheary elements. In contrast, when juvenile leaves were used, transdifferentiation was first observed on d 3 and the percentage reached 30% (Fukuda and Komamine, 1980). Collectively, these two examples of transdifferentiation, namely PP TCs in *Arabidopsis* and tracheary elements in *Zinnia*, link shoot age and the competency of differentiated cells to transdifferentiate to a new cell fate.

Recently, Zhang et al. (2015) demonstrated that in *Arabidopsis* and tobacco (*Nicotiana*), the capacity to regenerate shoots from explants of leaves progressively declined from juvenile to adult leaves, and that this process is regulated by *SPL9*-group genes. Consistent with a role for *SPL9*-group, but not *SPL3*-group genes in regulating shoot regeneration (Zhang et al., 2015), our data showed a stronger negative correlation between PP TC development and *SPL9*, *SPL10*, and *SPL15* expression, compared to the levels of the *SPL3* transcript (Figs. 5, 7, and 8). *SPL9*-group genes exert their effects in repressing regenerative capacity of adult tissue by directly inhibiting the transcriptional activity of a group

of *B-type* *ARR* genes (Zhang et al., 2015). Given the apparent correlation between transdifferentiation of PP TCs and shoot regenerative capacity of leaves and a role for *SPL9*-group genes in regulating these processes, investigating the cytokinin signaling pathways associated with *B-type* *ARRs* is a promising avenue for future study of PP TC development in *Arabidopsis*.

Establishment of Heteroblastic Variations in PP TC Development as a Reference for PP TC Study in *Arabidopsis*

Previous studies of PP TCs in *Arabidopsis* (Maeda et al., 2006, 2008; Amiard et al., 2007) typically examined fully expanded or so-called mature leaves, without awareness of the heteroblastic aspects of PP TC development reported here. Consequently, in light of our findings, it is imperative that comparisons in PP TC development in various experiments, such as between control and treatment, or wild type and mutants, need to be made in leaves harvested from the same node on the shoot given the differences seen in PP TC development even between successive leaves in the ecotypes assessed here (Fig. 1). Furthermore, careful analysis of the maturation status of individual leaves is an important consideration given that wall ingrowth abundance increases with leaf maturation, with the degree of such increase being different in individual leaf identities (Fig. 4). Given these observations, it is preferable to analyze PP TCs in mature leaves rather than developing leaves to minimize variations seen in the on-going formation of wall ingrowth networks. If mature transition or adult leaves are selected for assessment of PP TC development, the location of the vascular bundles within the leaf also needs to be considered, because wall ingrowth abundance decreases from tip to base in these leaves, and does so more dramatically in adult leaves (Figs. 1, 2, C, D, G, H, K, and L, and 5E). Furthermore, in a given PP TC, wall ingrowth abundance can also vary considerably in different areas along the cell wall that abuts the SE/CC complex (e.g. Fig. 2, A, C, E, and K). In this context, the robustness of the mPS-PI staining technique (Truernit et al., 2008) we have applied for confocal imaging of wall ingrowth deposition in PP TCs represents a substantially improved approach compared to ultrathin sectioning and TEM (Haritatos et al., 2000; Maeda et al., 2006, 2008; Amiard et al., 2007). Using this approach, we have mapped the distribution of PP TCs along the shoot axis (Fig. 1) and this map can now serve as a reference for future study of PP TC development in *Arabidopsis*.

Reevaluating Physiological Role(s) of Wall Ingrowth Deposition in PP TCs

It is widely accepted that immature leaves are sink tissues whereas mature leaves function as source organs delivering sugars to sinks via phloem loading

(Turgeon 1989, 2006). Therefore, an increase in PP TC abundance in mature leaves relative to that in immature leaves was initially considered to support a role for wall ingrowths in PP TCs facilitating phloem loading (Nguyen and McCurdy 2015), as previously suggested by others (Haritatos et al., 2000; Maeda et al., 2006). However, the observations reported here show that PP TC development in mature adult leaves is dramatically reduced compared to that in mature juvenile leaves (Fig. 4), although these leaves of both identities were fully expanded and hence potentially acting as source organs. This observation implies that PP TC development may not simply correlate with the source/sink status of leaves. This said, however, it is unknown whether photosynthetic rate of a leaf, and hence phloem loading capacity of minor veins, is similar between mature juvenile and mature adult leaves. In soybean, Yoshikawa et al. (2013) showed that photosynthetic rates were comparable between juvenile leaves 1 and 2 and adult leaves 4 to 7, albeit for an unusual increase in leaf 3. In contrast, in rice (Asai et al., 2002) and ivy (*Hedera*; Bauer and Bauer, 1980), photosynthetic activities are higher in adult leaves compared to juvenile leaves. As far as we are aware, there is no published work in *Arabidopsis* comparing photosynthetic rates of juvenile and adult leaves. However, Stessman et al. (2002) reported a remarkable decline in photosynthetic rate across maturation of leaf 8 in plants grown under continuous light. This decline in photosynthesis with leaf maturation is opposite to the observed increase in wall ingrowth abundance in PP TCs in each individual leaf (Fig. 4). Therefore, taken collectively, these observations call into question a primary role for wall ingrowth deposition in PP TCs in influencing phloem loading capacity.

Several articles have suggested a role in pathogen defense for wall ingrowth deposition in PP TCs. PP is often the primary target of phloem-feeding pathogens (Ding et al., 1998; Zhou et al., 2002), hence the bulky and highly localized deposition of wall ingrowths in PP TCs adjacent to SEs may act as a physical barrier to impede systemic pathogen spread (Amiard et al., 2007). This possibility is supported by the observations that the extent of wall ingrowth deposition in PP TCs can be triggered by the defense hormone jasmonic acid (JA; Amiard et al., 2007; Demmig-Adams et al., 2013), and that aphids, the major group of phloem-feeding insects, activate JA-mediated defense pathways (Louis et al., 2012) and stimulate cell wall modifications (Divol et al., 2005). In contrast to this result, wall ingrowth deposition in CC TCs in pea (*Pisum sativum*) leaf veins was not enhanced by exogenous methyl jasmonate, consistent with these wall ingrowths serving a primary role in enhancing phloem loading capacity (Wimmers and Turgeon, 1991; Amiard et al., 2007). Interestingly, of the large number of species showing TCs in collection phloem (either CC TCs, PP TCs, or both), only approximately 3% of this number have PP TCs alone (Pate and Gunning, 1969). Of this small number, the two species in which PP TCs are well documented, namely

Hare's foot plantain (*Plantago lagopus*; Pate and Gunning, 1969) and *Arabidopsis* (Haritatos et al., 2000), both display a rosette growth habit, with early emerged leaves (juvenile leaves in the case of *Arabidopsis*) being in close contact with soil and hence potentially prone to soil-borne bacterial and fungal infections. Consequently, the massive levels of wall ingrowth deposition seen in PP TCs in mature juvenile leaves (this study) and cotyledons of *Arabidopsis* (Nguyen and McCurdy, 2015) may provide a physical means of defense against pathogen attack.

MATERIALS AND METHODS

Plant Materials, Growth, and Growth Analysis

Arabidopsis (*Arabidopsis thaliana* (L.) Heynh. ecotype Columbia (Col-0) was used as wild-type reference for all mutants and transgenic lines. Col-0, *Ler-0*, *Ws-2*, *spl9-4* (CS67866), *spl15-1* (CS67867), *spl9-4/spl15-1* (CS67865), *zip-2* (CS24282), *rdm6-11* (CS24285), and *sgs3-11* (CS24289) lines were obtained from the *Arabidopsis* Biological Resource Center (Columbus, OH). *35S::MIM156* (Yu et al., 2013) and *35S::MIR156a* (Wu and Poethig, 2006) lines were kindly provided by J.-W. Wang and R.S. Poethig, respectively. The *sqm-6* and *SPL15-1D* mutants (Usami et al., 2009) were kindly provided by H. Tsukaya. *rSPL3*, *rSPL9*, and *rSLP10* (Zhang et al., 2015) were kind gifts from J.-W. Wang and T.Q. Zhang. For all experiments, seeds were sown directly onto pasteurized soil mix and stratified for 3 d in darkness at 4°C. Plants were then transferred to a growth cabinet with light supplied at 100 to 120 $\mu\text{mol m}^{-2} \text{s}^{-1}$, 22°C d/18°C night, 16 h photoperiod. These long-day conditions were used in all experiments, except for that presented in Supplemental Figure S5, where short-day conditions (8 h photoperiod) were used.

Numbers of juvenile and adult leaves and total leaf number were counted at bolting stage of plants. Abaxial trichomes were scored using a stereomicroscope at 3 to 4 weeks after planting and/or before leaves were subjected to fixation for mPS-PI staining. Leaf blade length and width, petiole length, and blade base angle were measured in fully expanded leaves using ImageJ 1.47m (<https://imagej.nih.gov/ij/>).

Defoliation Assays

Leaves 1 and 2 of 10-d-old Col-0 plants were removed using fine scissors and leaf removal was repeated at 2- or 3-d intervals until a total of 8 leaves were ablated. Leaves 9 or 10 from control and defoliated plants at maturation status of development were subjected to analyses of (1) PP TC development and (2) phase-specific traits including abaxial trichomes, blade length-to-width ratio, petiole-to-blade length ratio, and blade base angle. Defoliation experiments ($n = 9$, $n = 10$, and $n = 12$) were performed three times with the same outcomes, and thus representative data from a single experiment is presented.

mPS-PI Staining, Confocal Microscopy, and PP/PP TC Assays

mPS-PI staining of leaves was performed according to Nguyen and McCurdy (2015). In brief, leaves were fixed overnight at 4°C in ethanol:acetic anhydride (3:1), washed in 70% (v/v) ethanol, and cleared in 25% (v/v) White King bleach [4% (v/v) effective hypochlorite concentration] for at least 3 h depending on leaf age. Cleared tissue was washed extensively in water and stained in pseudo-Schiff propidium iodide (100 mM $\text{Na}_2\text{S}_2\text{O}_5$, 0.15 N HCl with propidium iodide added to a final concentration of 100 $\mu\text{g}/\text{mL}$) for at least 1 h. Stained leaves were mounted in a chloral hydrate mixture (4 g chloral hydrate, 1 mL glycerol, 2 mL water). Confocal imaging of mPS-PI stained leaves was performed using a FluoView FV1000 laser scanning confocal microscope (Olympus). Imaging used 488 nm Argon-ion laser excitation and emission wavelengths were collected at 522 to 622 nm. Semiquantitative analysis of PP TC development was performed as described in Nguyen and McCurdy (2015; and see Supplemental Fig. S1). Diameters of PP/PP TCs were measured using the scale bar tool of the FV1000 confocal microscope (Olympus).

Real-Time Quantitative RT-PCR

Real-time quantitative RT-PCR (RT-qPCR) with SYBR Green detection is described in Supplemental Materials and Methods. In brief, total RNA extracted using TRIzol (Life Technologies) from leaves at developmental stages corresponding to those of mPS-PI stained leaves was subjected to RT-qPCR using a specific protocol for parallel quantification of small and large RNA species (Speth and Laubinger, 2014). miR156 and miR172 levels were quantified relative to U6, while *SPL* expression was determined relative to two novel reference genes, *AT1G79810* (Peroxin 2) and *AT2G20790* (clathrin adaptor complexes medium subunit family protein). Expression stability of these controls was validated using geNorm (Vandesompele et al., 2002) and NormFinder (Andersen et al., 2004) algorithms. The quantitative cycle was determined using the Cy0 method (Guescini et al., 2008); the amount of target transcript was related to that of internal controls using the Livak method (Livak and Schmittgen, 2001). A full description of these methods is provided in Supplemental Materials and Methods. Primers used for RT-qPCR are listed in Supplemental Table S2.

Supplemental Data

The following supplemental materials are available.

Supplemental Figure S1. Confocal images of five classes of PP and PP TCs based on wall ingrowth abundance.

Supplemental Figure S2. Heteroblastic variations in three ecotypes: Col-0, *Ws-2*, and *Ler-0*.

Supplemental Figure S3. Rejuvenation of internal anatomical traits in leaf 10 upon prolonged defoliation.

Supplemental Figure S4. Confocal imaging of tracheary elements in mature leaf veins.

Supplemental Figure S5. Heteroblastic features of Col-0 plants grown under short-d conditions.

Supplemental Figure S6. Effects of *sqn-6* on VPC traits.

Supplemental Figure S7. Leaf morphology of 35S::*MIM156* and 35S::*MIR156* transgenic lines.

Supplemental Figure S8. Leaf morphology and the leaf position at which abaxial trichomes were first produced in Col-0, *zip-2*, *rdr6-11*, and *sgs3-11* plants.

Supplemental Table S1. Variations on number of abaxial trichomes and total leaf number of 35S::*MIM156* transgenic line.

Supplemental Table S2. List of primers used for RT-qPCR.

Supplemental Materials and Methods. Real-time quantitative RT-PCR.

ACKNOWLEDGMENTS

We thank the following for supplying seed lines: ABRC (Columbus, OH), Prof. R. Scott Poethig (University of Pennsylvania, Philadelphia, PA), Prof. Jia-Wei Wang (Shanghai Institutes for Biological Sciences, China), and Prof. Hirokazu Tsukaya (The University of Tokyo, Japan). We thank Dr. Renato Panebianco and the Cy0 team (University of Urbino Carlo Bo, Italy) for processing qPCR data using their Cy0 method and algorithms (Guescini et al., 2008), and thank Dr. Andy Eamens (The University of Newcastle, Australia) for comments on the manuscript. We thank Yuzhou Wu and Joe Enright for help with plant care.

Received November 15, 2016; accepted January 10, 2017; published January 12, 2017.

LITERATURE CITED

Amiard V, Demmig-Adams B, Mueh KE, Turgeon R, Combs AF, Adams III WW (2007) Role of light and jasmonic acid signaling in regulating foliar phloem cell wall ingrowth development. *New Phytol* **173**: 722–731

Andersen CL, Jensen JL, Orntoft TF (2004) Normalization of real-time quantitative reverse transcription-PCR data: a model-based variance estimation approach to identify genes suited for normalization, applied to bladder and colon cancer data sets. *Cancer Res* **64**: 5245–5250

Asai K, Satoh N, Sasaki H, Satoh H, Nagato Y (2002) A rice heterochronic mutant, *mori1*, is defective in the juvenile-adult phase change. *Development* **129**: 265–273

Berardini TZ, Bollman K, Sun H, Poethig RS (2001) Regulation of vegetative phase change in *Arabidopsis thaliana* by cyclophilin 40. *Science* **291**: 2405–2407

Bauer H, Bauer U (1980) Photosynthesis in leaves of the juvenile and adult phase of ivy (*Hedera helix*). *Plant Physiol* **49**: 366–372

Chen LQ, Qu XQ, Hou BH, Sosso D, Osorio S, Fernie AR, Frommer WB (2012) Sucrose efflux mediated by SWEET proteins as a key step for phloem transport. *Science* **335**: 207–211

Clarke JH, Tack D, Findlay K, Van Montagu M, Van Lijsebettens M (1999) The *SERRATE* locus controls the formation of the early juvenile leaves and phase length in *Arabidopsis*. *Plant J* **20**: 493–501

Demmig-Adams B, Cohu CM, Amiard V, van Zadelhoff G, Veldink GA, Muller O, Adams WW (2013) Emerging trade-offs—impact of photo-protectants (PsbS, xanthophylls, and vitamin E) on oxylipins as regulators of development and defense. *New Phytol* **197**: 720–729

Deng W, Ying H, Helliwell CA, Taylor JM, Peacock WJ, Dennis ES (2011) FLOWERING LOCUS C (FLC) regulates development pathways throughout the life cycle of *Arabidopsis*. *Proc Natl Acad Sci USA* **108**: 6680–6685

Ding XS, Carter SA, Deom CM, Nelson RS (1998) Tobamovirus and potyvirus accumulation in minor veins of inoculated leaves from representatives of the Solanaceae and Fabaceae. *Plant Physiol* **116**: 125–136

Divol F, Vilaine F, Thibivilliers S, Amselem J, Palauqui JC, Kusiak C, Dinant S (2005) Systemic response to aphid infestation by *Myzus persicae* in the phloem of *Apium graveolens*. *Plant Mol Biol* **57**: 517–540

Franco-Zorrilla JM, Valli A, Todesco M, Mateos I, Puga MI, Rubio-Somoza I, Leyva A, Weigel D, Garcia JA, Paz-Ares J (2007) Target mimicry provides a new mechanism for regulation of microRNA activity. *Nat Genet* **39**: 1033–1037

Fukuda H (2004) Signals that control plant vascular cell differentiation. *Nat Rev Mol Cell Biol* **5**: 379–391

Fukuda H, Komamine A (1980) Establishment of an experimental system for the tracheary element differentiation from single cells isolated from the mesophyll of *Zinnia elegans*. *Plant Physiol* **65**: 57–60

Gou JY, Felippes FF, Liu CJ, Weigel D, Wang JW (2011) Negative regulation of anthocyanin biosynthesis in *Arabidopsis* by a miR156-targeted SPL transcription factor. *Plant Cell* **23**: 1512–1522

Guescini M, Sisti D, Rocchi MBL, Stocchi L, Stocchi V (2008) A new real-time PCR method to overcome significant quantitative inaccuracy due to slight amplification inhibition. *BMC Bioinformatics* **9**: 326

Gunning BES (1977) Transfer cells and their roles in transport of solutes in plants. *Sci Progress (Oxford)* **64**: 539–568

Gunning BES, Pate JS (1974) Transfer cells. In AW Robards, ed, *Dynamic Aspects of Plant Ultrastructure*. McGraw-Hill, London, UK, pp 441–479

Gunning BES, Pate JS (1969) “Transfer cells”—plant cells with wall ingrowths, specialized in relation to short distance transport of solutes—their occurrence, structure, and development. *Protoplasma* **68**: 107–133

Gunning BES, Pate JS, Briarty LG (1968) Specialized “transfer cells” in minor veins of leaves and their possible significance in phloem translocation. *J Cell Biol* **37**: C7–C12

Haritatos E, Medville R, Turgeon R (2000) Minor vein structure and sugar transport in *Arabidopsis thaliana*. *Planta* **211**: 105–111

Hunter C, Sun H, Poethig RS (2003) The *Arabidopsis* heterochronic gene *ZIPPY* is an ARGONAUTE family member. *Curr Biol* **13**: 1734–1739

Hunter C, Willmann MR, Wu G, Yoshikawa M, de la Luz Gutierrez-Nava M, Poethig SR (2006) Trans-acting siRNA-mediated repression of ETTIN and ARF4 regulates heteroblasty in *Arabidopsis*. *Development* **133**: 2973–2981

Kerstetter RA, Poethig RS (1998) The specification of leaf identity during shoot development. *Annu Rev Cell Dev Biol* **14**: 373–398

Li S, Yang X, Wu F, He Y (2012) HYL1 controls the miR156-mediated juvenile phase of vegetative growth. *J Exp Bot* **63**: 2787–2798

Libby WJ, Hood JV (1976) Juvenility in hedged radiata pine. *Acta Hort* **56**: 91–98

Livak KJ, Schmittgen TD (2001) Analysis of relative gene expression data using real-time quantitative PCR and the $2^{-\Delta\Delta CT}$ method. *Methods* **25**: 402–408

Lobbes D, Rallapalli G, Schmidt DD, Martin C, Clarke J (2006) SERRATE: a new player on the plant microRNA scene. *EMBO Rep* **7**: 1052–1058

Louis J, Singh V, Shah J (2012) *Arabidopsis thaliana*-aphid interaction. *Arabidopsis Book* **10**: e0159

- Lu C, Fedoroff N (2000) A mutation in the Arabidopsis *HYL1* gene encoding a dsRNA binding protein affects responses to abscisic acid, auxin, and cytokinin. *Plant Cell* **12**: 2351–2366
- Maeda H, Sage TL, Isaac G, Welti R, Dellapenna D (2008) Tocopherols modulate extraplastidic polyunsaturated fatty acid metabolism in Arabidopsis at low temperature. *Plant Cell* **20**: 452–470
- Maeda H, Song W, Sage TL, DellaPenna D (2006) Tocopherols play a crucial role in low-temperature adaptation and Phloem loading in Arabidopsis. *Plant Cell* **18**: 2710–2732
- McCurdy DW (2015) Transfer cells—novel cell types with unique wall ingrowth architecture designed for optimized nutrient transport. In H Fukuda, ed, *Plant Cell Patterning and Cell Shape*. Wiley, Hoboken, NJ, pp 287–317
- Nguyen STT, McCurdy DW (2015) High-resolution confocal imaging of wall ingrowth deposition in plant transfer cells: semi-quantitative analysis of phloem parenchyma transfer cell development in leaf minor veins of Arabidopsis. *BMC Plant Biol* **15**: 109
- Nguyen STT, McCurdy DW (2016) Transdifferentiation—a plant perspective. In RJ Rose, ed, *Molecular Cell Biology of the Growth and Differentiation of Plant Cells*. CRC Press, Boca Raton, FL, pp 298–319
- Njoku E (1956) The effect of defoliation on leaf shape in *Ipomoea caerulea*. *New Phytol* **55**: 213–228
- Offler CE, McCurdy DW, Patrick JW, Talbot MJ (2003) Transfer cells: cells specialized for a special purpose. *Annu Rev Plant Biol* **54**: 431–454
- Okada TS (1991) Transdifferentiation: Flexibility in Cell Differentiation. Clarendon Press, Oxford, UK
- Orkiszewski JA, Poethig RS (2000) Phase identity of the maize leaf is determined after leaf initiation. *Proc Natl Acad Sci USA* **97**: 10631–10636
- Park MY, Wu G, Gonzalez-Sulser A, Vaucheret H, Poethig RS (2005) Nuclear processing and export of microRNAs in Arabidopsis. *Proc Natl Acad Sci USA* **102**: 3691–3696
- Pate JS, Gunning BES (1972) Transfer cells. *Annu Rev Plant Physiol* **23**: 173–196
- Pate JS, Gunning BES (1969) Vascular transfer cells in Angiosperm leaves: a taxonomic and morphological survey. *Protoplasma* **68**: 135–156
- Peragine A, Yoshikawa M, Wu G, Albrecht HL, Poethig RS (2004) *SGS3* and *SGS2/SDE1/RDR6* are required for juvenile development and the production of *trans*-acting siRNAs in Arabidopsis. *Genes Dev* **18**: 2368–2379
- Poethig RS (1990) Phase change and the regulation of shoot morphogenesis in plants. *Science* **250**: 923–930
- Schikora A, Schmidt W (2002) Formation of transfer cells and H⁺-ATPase expression in tomato roots under P and Fe deficiency. *Planta* **215**: 304–311
- Schuetz M, Smith R, Ellis B (2013) Xylem tissue specification, patterning, and differentiation mechanisms. *J Exp Bot* **64**: 11–31
- Schwab R, Palatnik JF, Riester M, Schommer C, Schmid M, Weigel D (2005) Specific effects of microRNAs on the plant transcriptome. *Dev Cell* **8**: 517–527
- Schwarz S, Grande AV, Bujdoso N, Saedler H, Huijser P (2008) The microRNA regulated SBP-box genes *SPL9* and *SPL15* control shoot maturation in Arabidopsis. *Plant Mol Biol* **67**: 183–195
- Smith MR, Willmann MR, Wu G, Berardini TZ, Moller B, Weijers D, Poethig RS (2009) Cyclophilin 40 is required for microRNA activity in Arabidopsis. *Proc Natl Acad Sci USA* **106**: 5424–5429
- Speth C, Laubinger S (2014) Rapid and parallel quantification of small and large RNA species. *Methods Mol Biol*. In D Staiger, ed, *Plant Circadian Networks: Methods and Protocols*, Methods in Molecular Biology. Springer, New York, vol. **1158**, pp 93–106.
- Stessman D, Miller A, Spalding M, Rodermeil S (2002) Regulation of photosynthesis during Arabidopsis leaf development in continuous light. *Photosynth Res* **72**: 27–37
- Telfer A, Bollman KM, Poethig RS (1997) Phase change and the regulation of trichome distribution in Arabidopsis thaliana. *Development* **124**: 645–654
- Telfer A, Poethig RS (1998) *HASTY*: a gene that regulates the timing of shoot maturation in Arabidopsis thaliana. *Development* **125**: 1889–1898
- Todesco M, Rubio-Somoza I, Paz-Ares J, Weigel D (2010) A collection of target mimics for comprehensive analysis of microRNA function in Arabidopsis thaliana. *PLoS Genet* **6**: e1001031
- Truernit E, Bauby H, Dubreucq B, Grandjean O, Runions J, Barthelemy J, Palauqui JC (2008) High-resolution whole-mount imaging of three-dimensional tissue organization and gene expression enables the study of phloem development and structure in Arabidopsis. *Plant Cell* **20**: 1494–1503
- Turgeon R (2006) Phloem loading: how leaves gain their independence. *Bioscience* **56**: 15–24
- Turgeon R (1989) The sink-source transition in leaves. *Annu Rev Plant Physiol Plant Mol Biol* **40**: 119–138
- Usami T, Horiguchi G, Yano S, Tsukaya H (2009) The *more and smaller cells* mutants of Arabidopsis thaliana identify novel roles for *SQUAMOSA PROMOTER BINDING PROTEIN-LIKE* genes in the control of heteroblasty. *Development* **136**: 955–964
- Vandesompele J, De Preter K, Pattyn F, Poppe B, van Roy N, De Paepe A, Speleman F (2002) Accurate normalization of real-time quantitative RT-PCR data by geometric averaging of multiple internal control genes. *Genome Biol* **3**: RESEARCH0034
- Vaughn KC, Talbot MJ, Offler CE, McCurdy DW (2007) Wall ingrowths in epidermal transfer cells of Vicia faba cotyledons are modified primary walls marked by localized accumulations of arabinogalactan proteins. *Plant Cell Physiol* **48**: 159–168
- Wang JW, Czech B, Weigel D (2009) miR156-regulated SPL transcription factors define an endogenous flowering pathway in Arabidopsis thaliana. *Cell* **138**: 738–749
- Wang JW, Park MY, Wang LJ, Koo Y, Chen XY, Weigel D, Poethig RS (2011) MiRNA control of vegetative phase change in trees. *PLoS Genet* **7**: e1002012
- Wang JW, Schwab R, Czech B, Mica E, Weigel D (2008) Dual effects of miR156-targeted SPL genes and *CYP78A5/KLUH* on plastochron length and organ size in Arabidopsis thaliana. *Plant Cell* **20**: 1231–1243
- Willmann MR, Poethig RS (2011) The effect of the floral repressor *FLC* on the timing and progression of vegetative phase change in Arabidopsis. *Development* **138**: 677–685
- Wimmers LE, Turgeon R (1991) Transfer cells and solute uptake in minor veins of Pisum sativum leaves. *Planta* **186**: 2–12
- Wu G, Park MY, Conway SR, Wang JW, Weigel D, Poethig RS (2009) The sequential action of miR156 and miR172 regulates developmental timing in Arabidopsis. *Cell* **138**: 750–759
- Wu G, Poethig RS (2006) Temporal regulation of shoot development in Arabidopsis thaliana by miR156 and its target *SPL3*. *Development* **133**: 3539–3547
- Wuyts N, Palauqui JC, Conejero G, Verdeil JL, Granier C, Massonnet C (2010) High-contrast three-dimensional imaging of the Arabidopsis leaf enables the analysis of cell dimensions in the epidermis and mesophyll. *Plant Methods* **6**: 17–30
- Xie K, Shen J, Hou X, Yao J, Li X, Xiao J, Xiong L (2012) Gradual increase of miR156 regulates temporal expression changes of numerous genes during leaf development in rice. *Plant Physiol* **158**: 1382–1394
- Xie K, Wu C, Xiong L (2006) Genomic organization, differential expression, and interaction of *SQUAMOSA* promoter-binding-like transcription factors and microRNA156 in rice. *Plant Physiol* **142**: 280–293
- Xing S, Salinas M, Höhmann S, Berndtgen R, Huijser P (2010) miR156-targeted and nontargeted SBP-box transcription factors act in concert to secure male fertility in Arabidopsis. *Plant Cell* **22**: 3935–3950
- Xu M, Hu T, Smith MR, Poethig RS (2016a) Epigenetic regulation of vegetative phase change in Arabidopsis. *Plant Cell* **28**: 28–41
- Xu M, Hu T, Zhao J, Park MY, Earley KW, Wu G, Yang L, Poethig RS (2016b) Developmental functions of miR156-regulated *SQUAMOSA PROMOTER BINDING PROTEIN-LIKE* (*SPL*) genes in Arabidopsis thaliana. *PLoS Genet* **12**: e1006263
- Yang L, Conway SR, Poethig RS (2011) Vegetative phase change is mediated by a leaf-derived signal that represses the transcription of miR156. *Development* **138**: 245–249
- Yang L, Xu M, Koo Y, He J, Poethig RS (2013) Sugar promotes vegetative phase change in Arabidopsis thaliana by repressing the expression of *MIR156A* and *MIR156C*. *eLife* **2**: e00260
- Yoshikawa T, Ozawa S, Sentoku N, Itoh J, Nagato Y, Yokoi S (2013) Change of shoot architecture during juvenile-to-adult phase transition in soybean. *Planta* **238**: 229–237
- Yu S, Cao L, Zhou CM, Zhang TQ, Lian H, Sun Y, Wu J, Huang J, Wang G, Wang JW (2013) Sugar is an endogenous cue for juvenile-to-adult phase transition in plants. *eLife* **2**: e0026
- Zhang TQ, Lian H, Tang H, Dolezal K, Zhou CM, Yu S, Chen JH, Chen Q, Liu H, Ljung K, Wang JW (2015) An intrinsic microRNA timer regulates progressive decline in shoot regenerative capacity in plants. *Plant Cell* **27**: 349–360
- Zhou CLE, El-Desouky A, Sheta H, Kelley S, Polek M, Ullman DE (2002) *Citrus tristeza virus* ultrastructure and associated cytopathology in *Citrus sinensis* and *Citrus aurantifolia*. *Can J Bot* **80**: 512–525